Aerodynamic Analysis of External Flow for

Hybrid Electric Vehicle (HEV)

by

Zulhazli Bin Baharum
1465
Mechanical Engineering

Dissertation submitted in partial fulfilment of the requirements for the
Bachelor of Engineering (Hons.)
(Mechanical Engineering)

JUNE 2004

Universiti Teknologi PETRONAS
Bandar Seri Iskandar
31750 Tronoh
Perak Darul Ridzuan

CERTIFICATION OF APPROVAL

Aerodynamic Analysis of External Flow for

Hybrid Electric Vehicle (HEV)

by

Zulhazli Bin Baharum

A project dissertation submitted to the
Mechanical Engineering Programme
Universiti Teknologi PETRONAS
In partial fulfillment of the requirement for the
BACHELOR OF ENGINEERING (Hons.)
(MECHANICAL ENGINEERING)

Approved by,

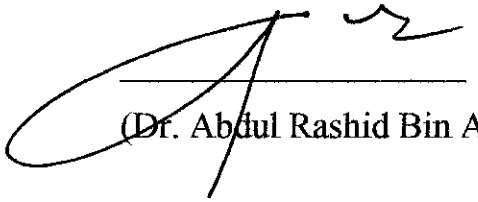

(Dr. Abdul Rashid Bin Abdul Aziz)

UNIVERSITI TEKNOLOGI PETRONAS
TRONOH, PERAK
JUNE 2004

CERTIFICATION OF ORIGINALITY

This is to certify that I am responsible for the work submitted in this project, that the original work is my own except as specified in the references and acknowledgements, and that the original work contained herein have not been undertaken or done by unspecified sources or persons.

ZULHAZLI BIN BAHARUM

ABSTRACT

The group goals and objectives are to design and construct a new design of aerodynamic interchangeable body and new vehicle architecture. The objective of the project at this stage is more on how to design vehicle shapes that produce desirable flow characteristic. Nevertheless, the pursuit of drag reduction remains one of the principal objectives. Theoretically, the shape of a moving vehicle causes the airflow to create force acting on the surface of the vehicle. The force is known as drag force. Therefore, by streamlining the vehicle body will help to reduce the effect of this force and increase its performance. Besides, the vehicle will have an attractive body design and minimized its fuel consumption.

The frontal area of a vehicle does influence the drag force exerted on the vehicle's body. The drag coefficient (C_D) depends mainly on the shape of the vehicle, regardless of their size or driving speed. Therefore, there is a relation between frontal area and the C_D, so that the vehicle with low C_D and A will experience much lower aerodynamic drag, and vice versa.

For this project, the important phases involve are the concept sketching, drawing and simulation analysis. The concept sketching is about the ideas that are being looked for, not refined designs. The selected concept was draw as a 3D drawing, using CATIA software. Finally, the drawing was used in computational fluid dynamics (CFD), using the STAR-CD software. STAR-CD is a powerful CFD tool and it has a built-in links with CAD/CAE systems. Several designs used in the CFD analysis and the result shows the pressure distribution, separation points as well as the wake generated at the rear of the vehicle. Various analysis and improvement of the design have been done, and as a result the value of C_D which is 0.14, has been obtained.

As a conclusion, the combination of underbody profiling, front, and rear end would lead to produce a vehicle shapes that produce desirable flow characteristic as well as possess low drag coefficient value.

ACKNOWLEDGEMENTS

I would like to express my greatest recognition and sincere appreciation to the ONLY Almighty God, ALLAH S.W.T. for giving me the strength and blessing, as well as the prophet Muhammad S.A.W. for his guidance.

The Final Year Project will not be a great successful to me without the Linear Generator (LG) Lab staff commitment and undivided supports. First and foremost, I would like to express my special gratitude to the project supervisor and co-supervisor, namely Dr. Abdul Rashid Abdul Aziz and Mr. Mohd Saifuddin Mohamad, for their precious guidance and consultation at all times throughout the course of this study.

I would also like to record my utmost appreciation to Associate Professor, Dr. Fakhruldin Mohd. Hashim, the Head of Mechanical Engineering Department, Mr. Saravanan Karuppanan and Mrs. Azuraien Jaafar, the Mechanical Engineering Programme Final Year Project Coordinator, for their patience, understanding and encouragement during the duration of this study. Special thanks to Mr. Mohd. Arief and Mr. Shiraz from the Mechanical Engineering Department for their consultation and assistance in the planning and strategizing of this study. A word of sincere gratitude to Mr. Mustafa, UTP R&D Engineer, for his cooperation and advices in the completion of this study.

Lat but not least, I would like to thank my family, all my friends and any individual who has contributed to the completion of this project in one way or another but has been inadvertently not mentioned.

TABLE OF CONTENTS

LIST OF FIGURES

LIST OF GRAPHS

CHAPTER 1

INTRODUCTION

1. INTRODUCTION

An aerodynamically efficient vehicle shape, possessing a very low drag coefficient (C_D), can help significantly in lowering fuel consumption. This is particularly true in cases such as at high speed operation. The worldwide trend, over the last three decades, the improvement of overall level of fuel efficiency for vehicles has been assisted by a trend to lower drag coefficients for private vehicle, especially.

1.1 Background

Aerodynamic road vehicles are basically about the design of a vehicle shapes that produce desirable flow characteristic of air, where it follows the contour of the body of the car. A road vehicle's shape is primarily determined by its functional, economic, and aesthetical value. In fact, aerodynamics does influence the design of car. There are several forms of drag exerted upon a car body when its moves through air. However, the important one that always being taken into consideration is the pressure drag.

In fluid mechanical terms, road vehicles are bluff bodies in very close proximity to the ground. The flow over the vehicle is fully three-dimensional. Flow separation is common and may be followed by reattachment. The boundary layers are turbulent, and large turbulent wakes and longitudinal trailing vortices are formed at the rear of the vehicle.

Drag coefficient C_D, can be used to determine the drag force on the vehicle. The continuous study over the aerodynamics in the automobile industry has lead to these five important events which affect the value of drag coefficient:

1. The recognition that the pattern of flow around half a body of revolution is changed significantly when that half body is brought close to the ground (Klemperer 1922).
2. The truncation of a body's rear end (Koenig-Fachsenfeld et al 1936).
3. The introduction of "detail-optimization" into vehicle development (Hucho et al 1976).
4. The deciphering of the detailed flow patterns at car rear ends.
5. The application of "add-ons" like underbody air dams, fairings, and wings to passenger cars, trucks, and race cars.

With these five steps, aerodynamics has been adapted to road vehicles and provides a better flow as well as lowering the drag exerted on the car. Furthermore, the aerodynamic body improves fuel economy of the car (less fuel consumption) and this had influence in the market situation. Fuel economy and, increasingly, global warming are the current key arguments for low drag coefficient, C_D.

1.2 Problem Statement

1.2.1 Drag coefficient and drag factor

The drag coefficient depends mainly on the shape of the vehicle, regardless of their size or driving speed. The drag coefficient thus provides a good indication of the relative merits of different vehicle shape. The symbol of this drag coefficient is C_D. From the equation of Drag Factor C_DA:

$$\text{Drag} = \tfrac{1}{2} \rho V^2 A C_D$$

Where, A is the frontal area

ρ is the density of the air

V is the speed of the vehicle relative to the air

The aerodynamic drag consists of drag coefficient, frontal area of the vehicle, the air density, and the square of the relative speed. As conclusion, vehicle with low C_D does not have low aerodynamic drag. As a conclusion, there is a relation between frontal area and the C_D, so that the vehicle with low C_D and A will experience much

lower aerodynamic drag, and vice versa. Even though the C_D is dependent on the turbulence properties of the flow and the Reynolds Number (varies with speed), the C_D can be treated as if it were a constant. For the normal range of road vehicle cruising speeds, the changes are usually insignificant.

The analytical difficulties arise from the fact that the flow around a road vehicle is highly three-dimensional, the air does not follow the contours of the body everywhere, and there is nearly always an unsteady wake. The important feature of the subject of road vehicle aerodynamics is that there are no straightforward methods for predicting how air will flow around a given vehicle shape. However, at present, nearly all aerodynamic design for road vehicles relies on a combination of experimental results (simulation analysis, wind-tunnel testing), and understanding of the way that air flows behave. It is still necessary to have an analytical basis for the methods used to treat the experimental data, to predict performance, and to relate wind-tunnel results to full-scale behavior.

Aerodynamic noise is due principally to pressure fluctuations associated with turbulence and vorticity. For road vehicle this can be separated into three noise generating components:

1. The boundary layer distributed over the vehicle body.
2. Edge effects.
3. Vortex shedding at various locations on the vehicle body.

Noise levels due to boundary layer effects are not normally troublesome. Boundary layer noise tends to be random in character and is spread over a broad band of frequencies. Edge noise is produced by flow separating from sharp corners and edges on the body structure. As the flow separates from an edge it rolls up into large vortices which also break up into smaller vortices. The noise level associated with edge noise is generally higher than boundary layer noise. Vortex shedding occurs when airflow strikes a bluff-body producing a periodic stream of vortices downstream. It is the most annoying of all sounds. The frequency f of the vortices is related to the air speed U and depth d of the bluff body by the equation:

- $f = \frac{SU}{d}$,where S is the Strouhal number.

1.3 Objectives and Scope of Study

The objective of the project at this stage is more on how to design vehicle shapes that produce desirable flow characteristic. Nevertheless, the pursuit of drag reduction remains one of the principal objectives. When viewed in totally, the aerodynamic efficiency of a vehicle arises not only from the basic shape of the vehicle, but also from its vast number of detailed geometries that interact with the exterior flow, such as the cooling air inlet, underbody components, etc.

There are several vehicle attributes affected by aerodynamics and one of them is the performance and fuel economy, as being explained earlier in this report. Another attributes is about the handling. Aerodynamic body with low C_L tends to apply more loads onto the tires and this will increased the grip of the tires itself. This is good for cornering and has tendency to avoid over steer, which is undesirable.

The scope of study for this project is to do research, design and development work especially on the vehicle body construction, in order to produce the practical solution. There will be an opportunity to use the tolls and techniques of problem-solving to solve the problems encountered and applying the management concepts which required skills for managing the whole project till the end.

Initially, several possible designs have been sketched in order to come out with the final design. These possible designs are being made through some research over the concepts of aerodynamic car and the latest/up-to-date design of private vehicles. Furthermore, these designs were made base on the dimension of a WIRA as being agree earlier among the group members and supervisor. However, only several parts are base on the WIRA's dimension such as the wheelbase, overall height, and ground clearance. The dimensions of other parts of the whole body are independent but still base on the aerodynamic analysis that being made.

After the discussion, one design was being picked up as the final design. At this stage, proper 3D drawing has to be made in order to run the aerodynamic analysis.

Several changes over the design were being made to meet the requirement and to reduce drag exerted on the vehicle, as it is the main objective of this project.

The research and design processes will be done throughout the first semester, and the fabricating process for the whole designing will be done in the second semester of Final Year. The whole processes of research and design an aerodynamic interchangeable body and new vehicle architecture will be divided into four (4) main parts which are:

i. Aerodynamic body design and analysis.
ii. Wind-Tunnel testing.
iii. Material selection for the outer body and constructing method.
iv. Material selection for the car's frame and constructing method.

All those designing processes above will be performed throughout the whole first semester of Final Year Project (FYP) and the construction of the whole body will be performed in the second semester. The author will be focusing more on the first part of the project, which is aerodynamic body design and analysis.

CHAPTER 2

LITERATURE REVIEW AND THEORY

2. LITERATURE REVIEW AND THEORY

2.1 Bernoulli's equation

The movement of the airflow near the body creates a velocity distribution which in turn creates the aerodynamic loads acting on the vehicle. These loads, in general, can be divided into two major contributors. The first is the shear (skin friction) force, which acts tangentially to the surface and contributes to drag. The second force is pressure, and it acts normal (perpendicular) to the surface and contributes to both lift and drag (so vehicle down force is really the added effect of the pressure distribution). The Bernoulli Equation describes the relation between air-speed and pressure:

$$\frac{p}{\rho} + \frac{V^2}{2} = \text{constant}$$, p=static pressure, ρ=density, V=velocity

In this equation, if airspeed varies as it flows around an object, then the pressure will change in an inverse proportion to the square of the airspeed. In other words, as the air flows faster around the vehicle, the pressure will be reduced.

2.2 Drag, Lift, and Side Force

The direction of the drag force is parallel to the vehicle's motion and points toward the back of the vehicle; the side force is pointed to the side of the vehicle; while the lift acts upward, normal to the ground. However, only drag and lift force are taken into consideration since the side force only important in cases of strong cross winds and when passing. Down force is equal to negative lift. The equations;

- Drag Coefficient: $C_D = \frac{D}{\frac{1}{2}\rho V^2 A}$ *(Eq. 2.21)*

- Lift Coefficient: $C_L = \frac{L}{\frac{1}{2}\rho V^2 A}$ *(Eq. 2.22)*
- Side force Coefficient: $CY = \frac{Y}{\frac{1}{2}\rho V^2 A}$ *(Eq. 2.23)*

2.3 Airfoils and Wings

An airfoil is the two-dimensional cross section of three-dimensional wing. A two-dimensional airfoil can be viewed as the cross section of a rectangular wing. The overall effect of the airfoil on the surrounding fluid results in a faster flow above it and a slower flow under it. According to Bernoulli's equation, because of this velocity difference the pressure above the airfoil will be lower than under it. The resultant force will act upward and is called lift.

2.3.1 Lift Coefficient of an Airfoil

The lift coefficient C_l of such an airfoil is defined and calculated per unit width of the airfoil. So, when using *Eq. 2.22*, the reference area becomes the chord c multiplied by a unit width:

$$C_l = \frac{l}{\frac{1}{2}\rho V^2 c} \qquad \textit{(Eq. 2.3.11)}$$

, l = lift per unit width.

The increase in the lift of a symmetric airfoil, as the angle of attack α increases, is given by the formula:

$$C_l = 2\Pi\alpha \qquad \textit{(Eq. 2.3.12)}$$

C_l is a non-dimensional number and α is measured by radians (multiplied by $\Pi/180$ for value in degree). For a cambered airfoil the coefficient 2Π does not change, but there is an increment in the effective angle of attack by α_{L0}. Thus, the symmetric airfoil will have zero lift at $\alpha=0$ while the cambered airfoil will have a lift of $C_l = 2\Pi$

$\alpha_{L0,}$ even at zero angle of attack. Consequently, for a cambered airfoil, equation above can be rewritten as:

$$C_l = 2\Pi (\alpha + \alpha_{L0}) \qquad \textit{(Eq. 2.3.13)}$$

The lift coefficient, C_l obtained here can be used in *Eq. 2.22* to obtain the actual lift force. The effect of thickness t /c is to slightly increase lift. Consequently, the modified form of Eq.*, for a thick airfoil is:

$C_l = 2\Pi (1 + 0.77\ t/c) \sin \alpha$, $\sin \alpha$ is used instead of α. *(Eq. 2.3.14)*

2.4 Effect of Pressure Gradient

If the pressure varies in the direction of flow then the behavior of the boundary layer flow may be greatly affected. If we consider the flow over a curved surface as in the figure below then between points A and C the flow is accelerated until at point C the velocity outside the boundary layer is a maximum, and the pressure is a minimum, the pressure gradient is therefore negative and the net pressure force on an element of fluid in the boundary layer is in the direction of flow.

This negative pressure gradient is said to be favorable. Beyond C however the pressure increases so the net force on an element will oppose the flow. Near the boundary where the fluid momentum is the lowest the pressure force will tend to bring the fluid to rest (D) or further downstream will actually reverse the flow. As the fluid is no longer able to follow the contours of the surface it breaks away. This is termed separation and the point at which it occurs (when $\delta u / \delta y$ becomes zero) as the separation point.

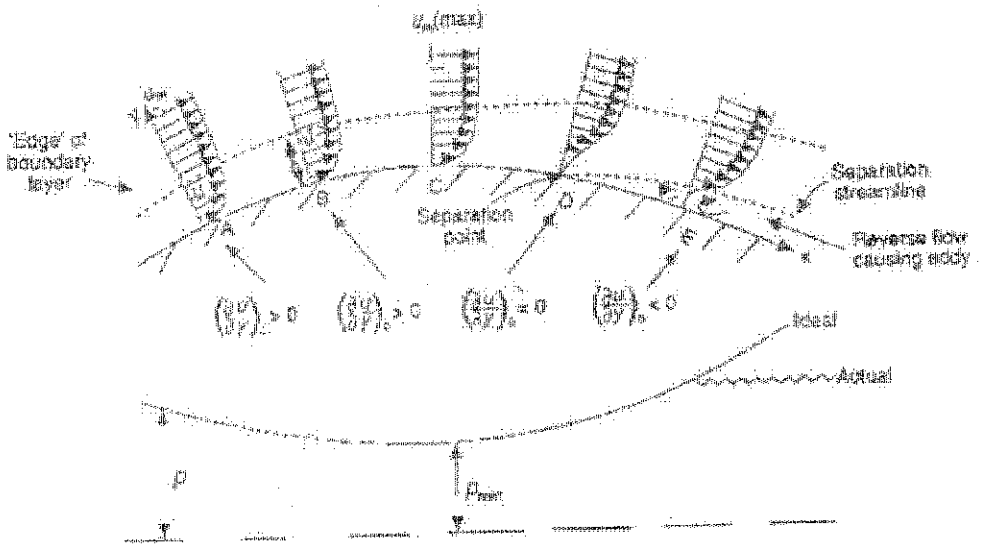

Figure 1: Effect of Pressure Gradient

Separation occurs in both laminar and turbulent boundary layers but laminar ones are more prone to separation because the increase of velocity with distance from the surface is less rapid. In the study of ground vehicles the behavior of the boundary layer is responsible for the form of the vortex development and the areas of separated flow on the vehicle.

2.5 Wake Development

An understanding of the behavior of the wake can be obtained by considering the flow past a long cylinder. For very low values of Reynolds number (Defined in terms of the diameter of the cylinder) say less than 0.5 the inertia forces are negligible and the streamlines come together behind the cylinder. In the range 2-30 the boundary layer separates symmetrically and two eddies form, however the main streamlines come together and the length of the wake is limited. With increasing Reynolds number the wake lengthens and at around Re = 40-7- becomes unstable so that a periodic oscillation of the wake occurs.

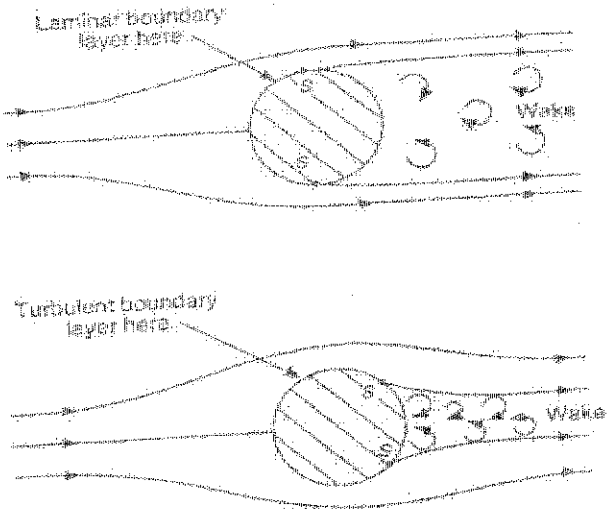

Figure 4: Wake of Laminar & Turbulent Layer

2.6 Effect of using incompressible flow equations on accuracy

In the case of 'normal' road vehicles, (this excludes speed record vehicles and possibly racing cars) it is assumed that the flow is incompressible. In this case the Bernoulli equation is valid and as the fluid is air we can ignore the position term (ρgz). The equation is then simplified to:

$$p + \tfrac{1}{2}\rho v^2 = \text{constant}$$

The validity of this assumption can be verified by developing the pressure / velocity / Mach number relation from the steady flow energy equation and the isentropic temperature pressure relationship.

$$\frac{Po}{p} = \left[1 + \frac{(\gamma-1)}{2} M^2\right]^{\gamma/(\gamma-1)}$$

Using the Binomial expansion:

$$(1+x)^n = 1 + nx + \frac{n(n-1)x^2}{2!} + \ldots\ldots$$

And the substitution,

$$p\gamma M^2 / 2 = \rho v^2 / 2$$

gives:

$$p_o = p + \tfrac{1}{2}\rho v^2 [\, 1 + M^2/4 + (2-\gamma)M^4/24 + \ldots\ldots]$$

The first two terms of the expansion are the same as the incompressible Bernoulli equation, the additional terms are therefore the error associated with using this equation. Substituting various values of the Mach number into the equation the error associated with using the incompressible form is shown to be:

M = 0.1 : 0.25%
M = 0.2 : 1.0%
M = 0.3 : 2.25%
M = 1.0 : 28.0%

The simplification afforded by the incompressible flow assumption is more than counterbalanced by the problems arising from:

- Ground proximity
- The 'bluff' shapes used which lead to strong viscous flow separation effects
- Effects due to ambient wind such as cross flow, the ground velocity gradient and the natural winds unsteady nature

2.7 Pressure Coefficient

It is convenient to investigate the pressure distribution around a given shape using a non-dimensional pressure coefficient. The figure below shows a schematic of the two dimensional inviscid flow around a vehicle, three stagnation points are present, on the nose of the vehicle, at the bottom of the windscreen, and at the rear of the vehicle. The pressure coefficient is defined as:

$$Cp = \frac{P - P_{atm}}{\tfrac{1}{2}\rho v^2_{atm}}$$

From the Bernoulli equation:

$$P_{atm} + \tfrac{1}{2}\rho v^2_{atm} = P + \tfrac{1}{2}\rho v^2$$

Rearranging

$$P - P_{atm} = \tfrac{1}{2}\rho v^2_{atm} - \tfrac{1}{2}\rho v^2$$

And hence:

$$Cp = 1 - [v^2/v^2_{atm}]$$

2.8 Calculation of aerodynamic pressure force

In the case of car shape, the approach is as follows. Consider the shape shown below.

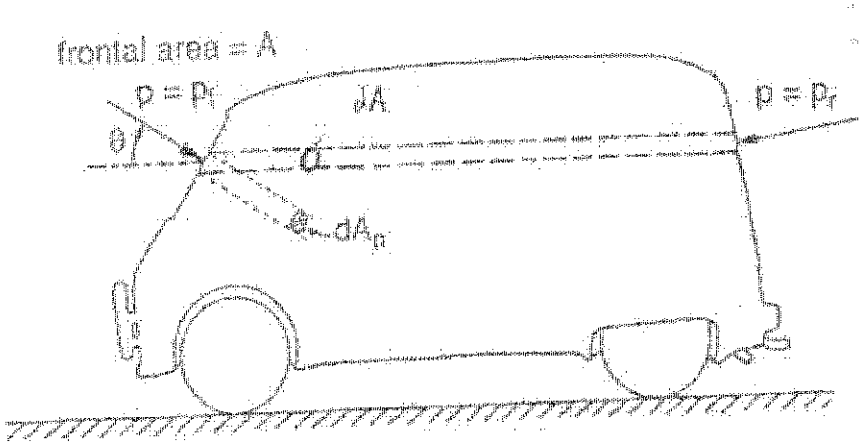

Figure 5: Example of a car shape for Aerodynamic calculation

The pressure force due to pressure p acting normal to the element *dAn* is *p.dAn*, and the drag component of this is *p.dAn*.cosθ. Alternatively if we consider an element *dA* of the projected frontal area, (i.e. $dA = dAn.\cos\theta$) then the drag force on the element is *p.dA*.

The pressure acting on the front facing surface of *dA* is p_f, and the pressure acting on the rear facing surface is p_r. The normal pressure force on this area is $(p_f p_r)dA$, therefore the total normal pressure drag is:

$$D_{np} = \int_A (p_f - p_r)dA = \int_A [(p_f - p_{atm}) - (p_r - p_{atm})]dA$$

However as,

$$C_p = \frac{P - P_{atm}}{\frac{1}{2}\rho v^2_{atm}}$$

Then,

$$D_{np} = \frac{1}{2}\rho v^2_{atm} \int_A (C_{pf} - C_{pr}) dA$$

For the purpose of calculating the normal pressure drag coefficient area weighted mean values of Cp are defined using the general formula:

$$\overline{C_p} = 1/A \int_A C_p \, dA$$

Hence the normal pressure drag force is given by:

$$D_{np} = \frac{1}{2}\rho v^2_{atm} (\overline{C_{pf}} - \overline{C_{pr}})$$

The normal pressure drag coefficient can be calculated using the definition for C_D, and it is noted that the areas cancel out because the frontal area is the reference area:

$$C_{Dnp} = \frac{Dnp}{\frac{1}{2}\rho A v^2_{atm}} = (C_{pf} - C_{pr})$$

A similar calculation can be performed to determine the lift and side forces but care should be taken when determining the coefficients as they too are defined using the frontal area, but the area weighted C_p's will be determined using plan and projected side areas.

CHAPTER 3

METHODOLOGY

3. METHODOLOGY

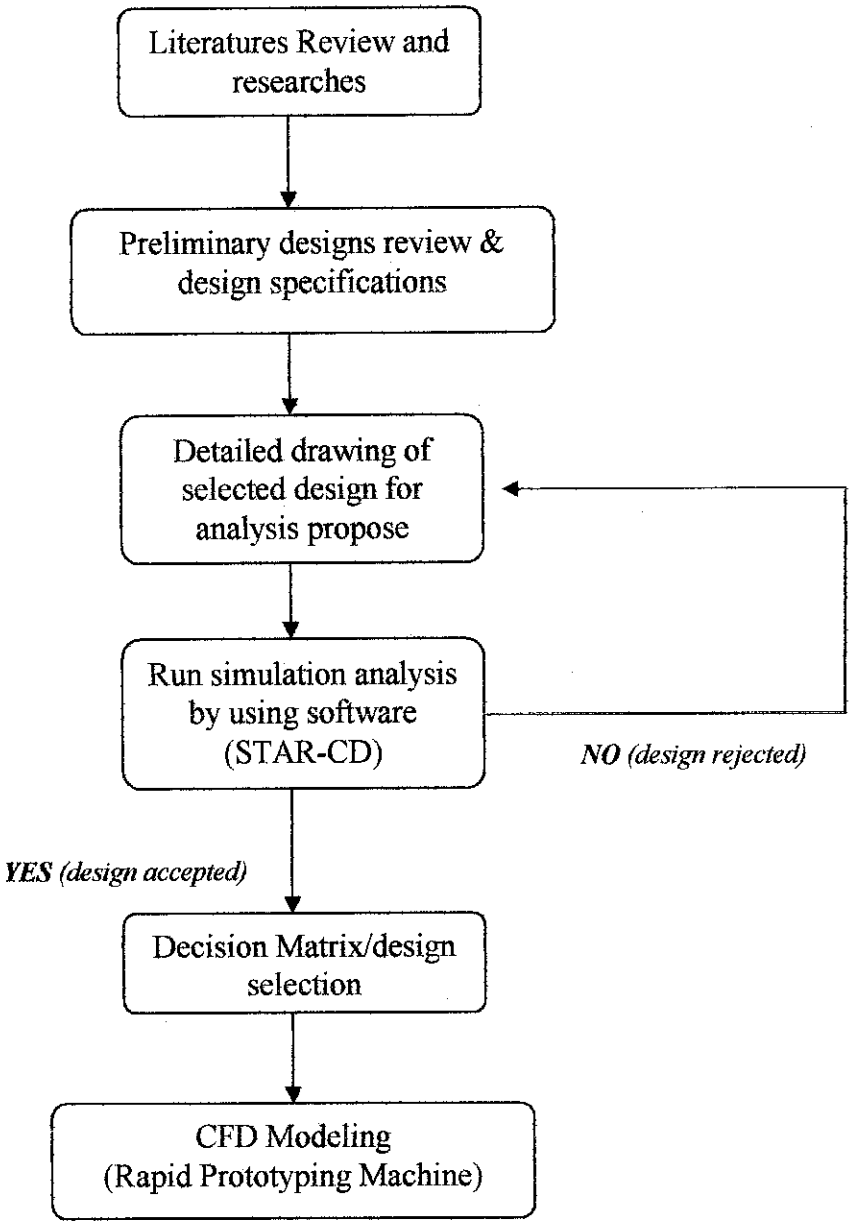

The tasks of the author for this project, which being emphasized are:

- Preliminary designs review and design specification.
- Detail drawing of the selected design for simulation analysis.
- Simulation analysis.

Basically, each phase should be followed step-by-sep which is, each phase cannot be done before finishing the previous phase. Below are the descriptions of each phase.

3.1 Preliminary designs review and design specification

The concept sketching is about the ideas that are being looked for, not refined designs. About more than 5 sketches have been drawn, and those sketches produced were loose and fairly unconstrained. Accuracy at this stage is not a prime requirement, a basic concept is. Base on the literatures review, several sketches were done as preliminary designs. The application of the mechanical and ergonomic requirements is partly included. The methods include creating designs on paper as 3D sketches.

As being mentioned earlier, the team responsibility is solely on the body of the vehicle. Basically, the generation of concept sketches is part of the stylist's job. Therefore, the concept sketches were done base on the observation, experience and interpretation, and much of the decision making over the car's concept and style is quite intuitive.

The purposes of these concept sketches are:

- To define what concept and style is applicable for the Hybrid Electric Vehicle; the body must not interfere with the parts or components of the Engine.
- The concept must have attractive value and look fast even when stands still.
- Fulfill the requirements such as it is a two passenger's car, interchangeable body, less parts, and look fast even when stands still.

Sketches are produced and selected, via a series of presentations and discussions, in order to create further development. This will achieve the progression to full size elevational views and onto the full size model. It has to be aware that good detail cannot save a bad design, but bad detail can ruin a good one.

3.2 Detail drawing of the selected design for simulation analysis

The package drawing is the industry's term for the three dimensional (3D) view, full sized orthogonal drawing which shows the basic mechanical and ergonomic requirements of the intended vehicle. It is supplied to all engineering areas involved.

Base on the design criteria selected in the previous phase, the complete 3D drawing was being prepared to create mock-up model for wind-tunnel testing. The CATIA software for 3D modeling is used for this purpose. This software is selected because of its feasibility, and the team has learned on how to use the software before. In order to produce vehicle package drawing information, the following will be included (at actual dimension):

a) Overall length, width and height
b) Wheelbase, and sizes of wheels and tyres
c) Ground clearance, front and rear overhang (measured from wheel centre)
d) Windscreen location and angle
e) Engine's components location (Generator, Motor, Battery, etc)
f) Legal parameters of all lights and signals
g) Minimum/maximum bumper heights and clearances
h) All the aerodynamic application (backlight angle, underbody plane, etc) for analysis purposes

The drawing process might be repeated at some part of the vehicle, base on the aerodynamic requirement until a good selection of design is achieved. However, the alteration can only be made after doing the simulation analysis, which is in the next stage after this. The goal is to come out with the final detailed Hybrid Electric Vehicle's drawing that can be used to produce the mock up model for wind-tunnel testing. The 3-D drawing of the model is shown below:

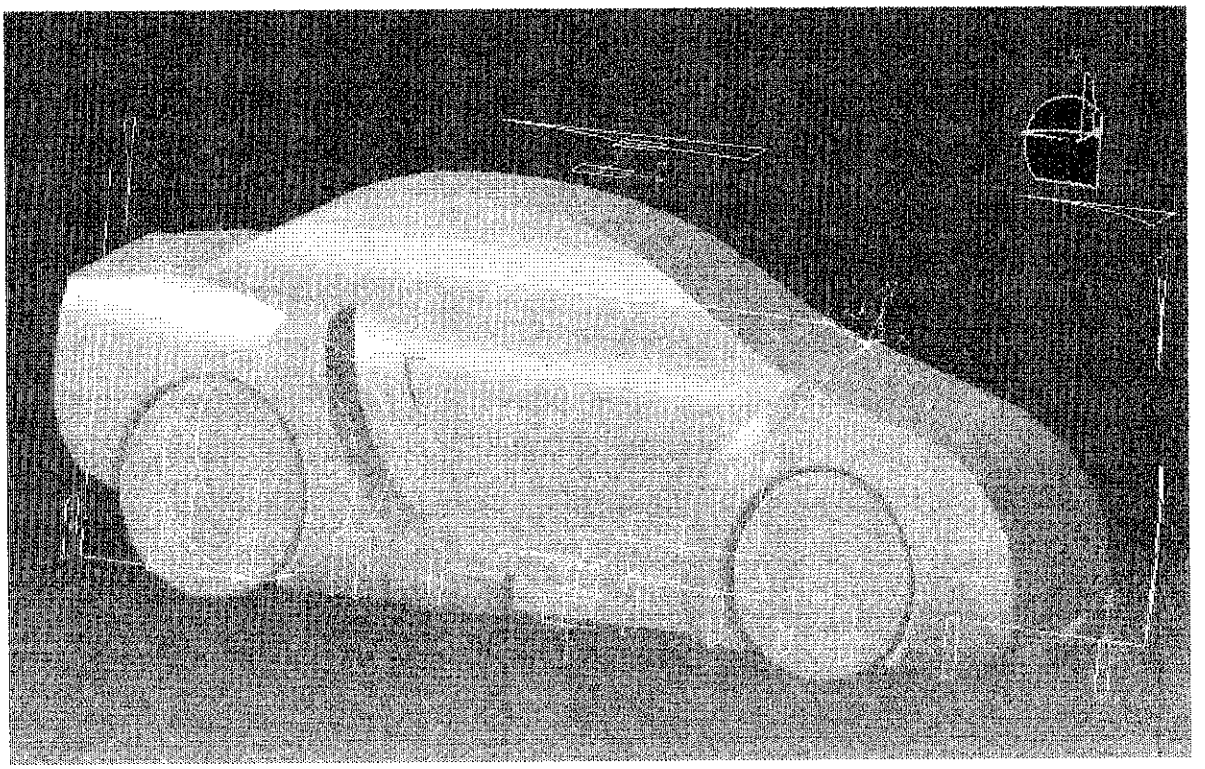

Figure 6: 3-D modeling

3.3 Simulation analysis

The STAR-CD software is used for the simulation analysis. This is a method of computational fluid dynamics (CFD) via simulation software. The STAR-CD is a powerful CFD tool and it has a built-in links with CAD/CAE systems. From this analysis, we could see the flow distribution over the vehicle's surface, the resulting drag coefficient (C_D), and the lift coefficient (C_L). The final design of the vehicle is mainly depends on the result of this analysis. Some significant changes might have to be made at certain parts of the vehicle, as being explain in the literatures review section, until the vehicle possessed low C_D and C_L values.

STAR-CD employs mathematical models of turbulence to determine the Reynolds stresses and turbulent scalar fluxes. These models comprise additional differential or algebraic equations that relate the aforementioned unknowns to selected ensemble-averaged properties of the turbulence field and also provide a framework for calculating these properties. Special models are also employed to characterize the flow near solid walls.

The main options currently available in STAR-CD for general applications are variants of the well known k-e model, all comprising transport equations for turbulent kinetic energy k and its dissipation rate e. the options differ from each other in one of the following respects:

- The form of the equations
- The treatment of the near-wall region
- The relation between Reynolds stresses and the rates of strain

CHAPTER 4

RESULT AND DISCUSSION

4. RESULT AND DISCUSSION

Recently, the progress in super computers and computational fluid dynamics (CFD) has motivated the CFD technology to be applied actively to the flow around a vehicle body. As being defined earlier in the literatures review's section, the aerodynamic characteristics of this body depended on the after body geometry, especially at the rear section. In order to examine reliability of computation, the computations were going to be performed with various parameters at the specific location. The flow around vehicle body can be assumed to be steady and incompressible. However, this is a first time exposure to the STAR-CD and there are a lot of thing needs to be defined before proceeding with the analysis. The computations will be done from time to time before come out with the final design of hybrid electric vehicle's body.

Experimental measurements of pressure distribution on the car body were also provided by the analysis. The mesh, partially shown in the figures, was generated with an in-house mesh generator (Please refer Figure 1 in Appendix II). It contains a total of 25 920 nodes in 19 736 cells. There are some amount of space provided at the front, side and rear of the car. The reason is to monitor the effects of the airflow around the car's body.
The molecular properties of air are:

- Density = 1.205 kg/m3
- Molecular viscosity = 1.81E -05 kg/ms

The inlet condition is in uniform velocity with magnitude of 27.78m/s and Reynolds number of 7.23×10^8. Normal atmospheric pressure (1 bar) was applied at the top boundary condition. A no-slip condition was applied on surfaces of the car body and

the ground. On the side boundaries, the stress free condition was used. An operator splitting algorithm [2] with variable time step was used. The High Reynolds k-epsilon model was employed for modeling the turbulence. STAR CD-PROSTAR iterative solver was used for this analysis. The mesh, partially shown in the figures, was generated with an in-house mesh generator. It contains a total of 25 920 nodes in 19 736 cells. There are some amount of space provided at the front, side and rear of the car. The reason is to monitor the effects of the airflow around the car's body. Figure of the meshing model is shown below.

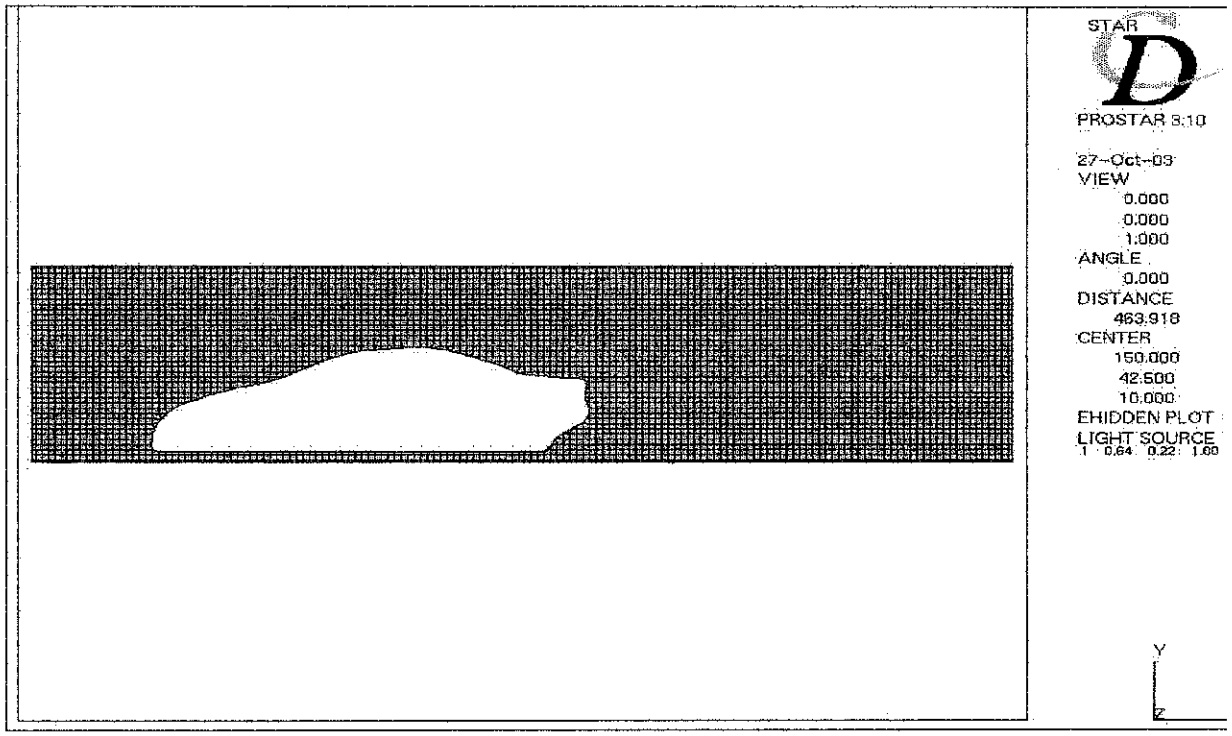

Figure 7: Mesh Generation

4.1 Initial Design

4.1.1 Pressure Distribution

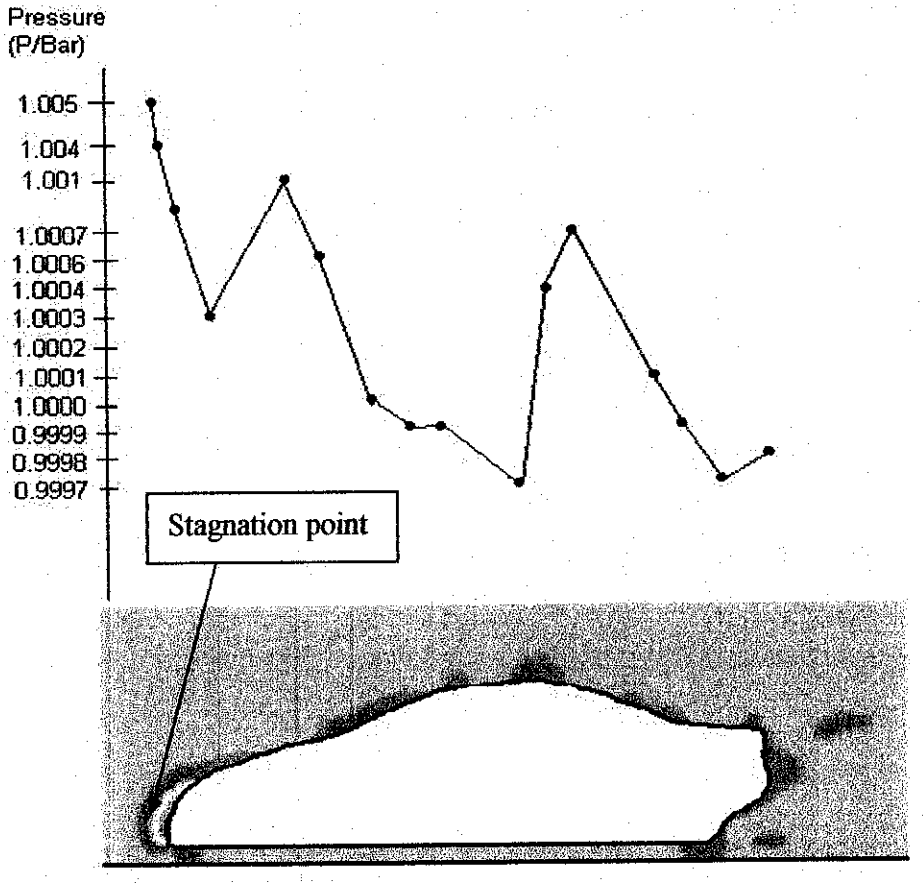

Figure 8: Centre-line pressure distribution of the vehicle

The figure above explained about the pressure distribution over the vehicle's body. This is the first design applied in this project. Basically, this analysis was done in the first semester of the project and the analysis is made to determine whether the selected design is applicable for further analysis. Theoretically, the pressure distribution obtained above is acceptable and all furthers analysis will be based on this model. From the above figure, we can notice that the pressure was at highest value, at the stagnation point of the vehicle.

Basically, the point where the air strikes the body, it momentarily comes to rest, and the position where it occurs is called a stagnation position. At this point, the air pressure will have its stagnation value, which is the maximum that it can attain anywhere in the flow. The great amount of stagnation (pressure) at the front of the model was due to large frontal area. There were also some stagnation on the front and rear windscreen. These

stagnation effect, cause an increase in pressure and therefore an increase in drag force. There is also a decrease in speed at the lip on the roof that can increase the pressure.

4.1.2 Velocity Profile

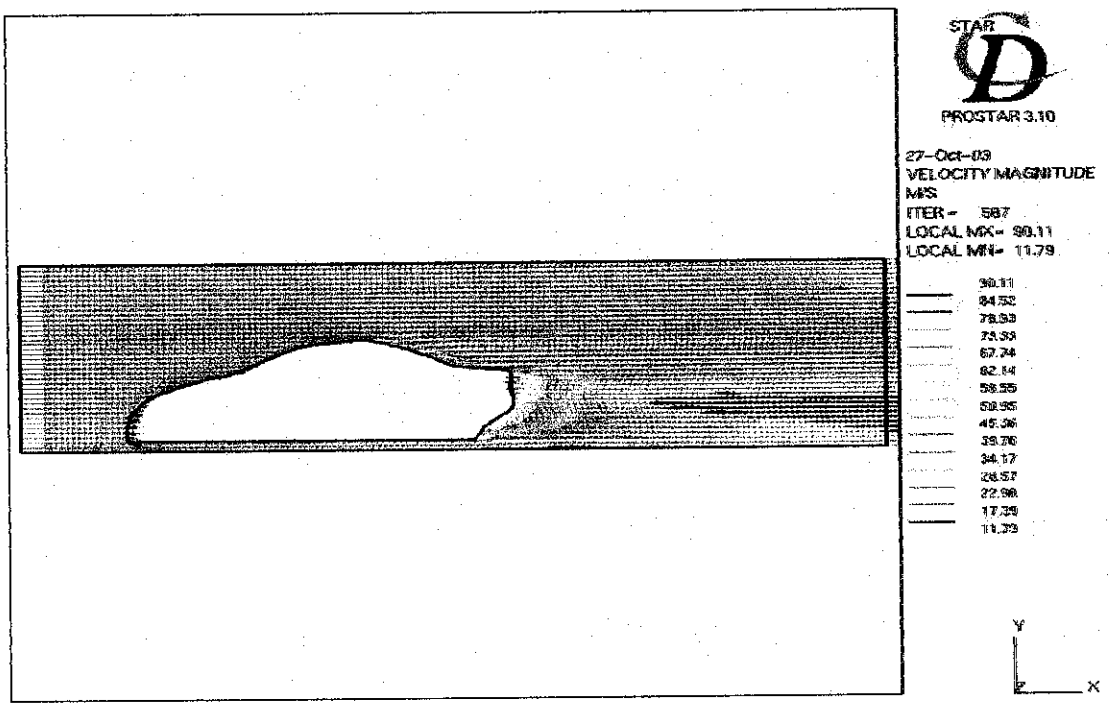

Figure 9: Velocity profile of the initial design

The figure above shows the velocity profile of the early design before some adjustment being made based on the result obtained in this analysis. One of the main parts that contribute to the high drag coefficient of any design of a car is at the rear part of it. Other crucial parts that contribute to high drag coefficient are the stagnation line and the underbody profiling of a car. From the figure below, it shows that there is a huge wake or unsteady flows formed due to the separation at the rear end of the car. There are several forms of counter rotating vertices with different velocity and it has affected the flows pattern of the air at the rear part of the vehicle.

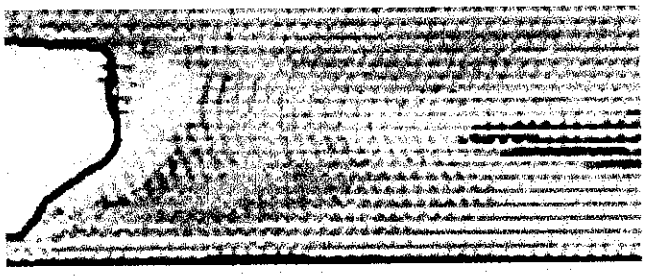

Figure 10: The wake region at the back of the initial design

4.2 Improvement of the design

4.2.1 Front End

Flat corner and sharp edge have the tendency to produce strong separations at the front area of the vehicle. Referring to Hucho, drag reductions can be produced (up to 14 per cent) by modest rounding and lowering of this corner.

Base from the data presented by Buchheim *et al.*, the drag coefficient is varies significantly by the height of front stagnation line. The lower the stagnation line, the lower drag coefficient value could be obtained. Additionally, low front stagnation line has the advantage to reduce the lift at the front. Therefore, three different parameter of stagnation line, Z_f have been applied on the model in order to obtain the lowest C_D value as possible. The parameters are:

1. 130 mm
2. 280 mm
3. 415 mm

The overall height, Z_b is 1385 mm. Therefore:

1. $\frac{Z_f}{Z_b} = 0.1$
2. $\frac{Z_f}{Z_b} = 0.2$
3. $\frac{Z_f}{Z_b} = 0.3$

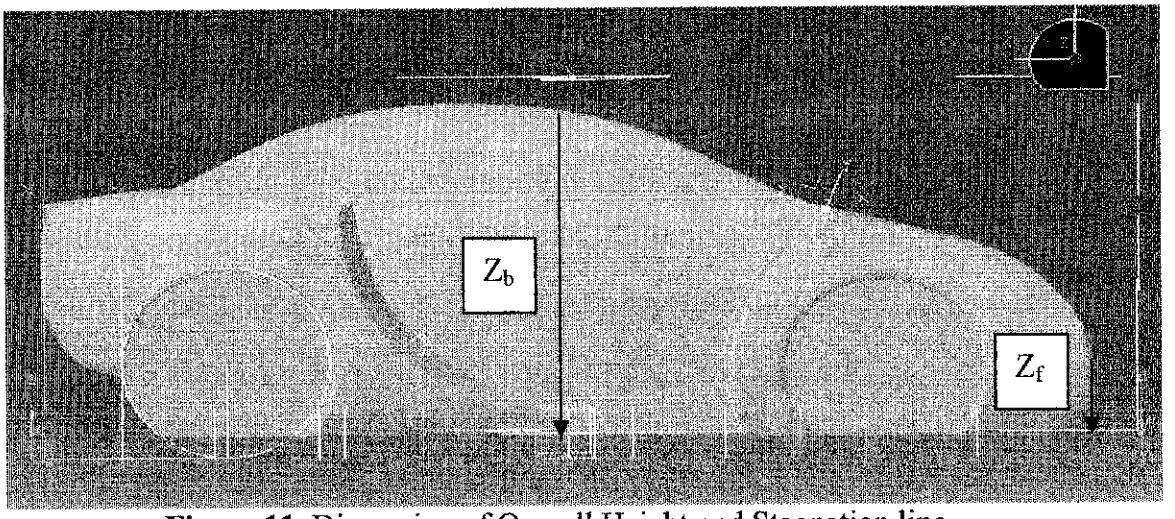

Figure 11: Dimension of Overall Height and Stagnation line

The graph below shows the distribution of drag coefficient obtained from the analysis:

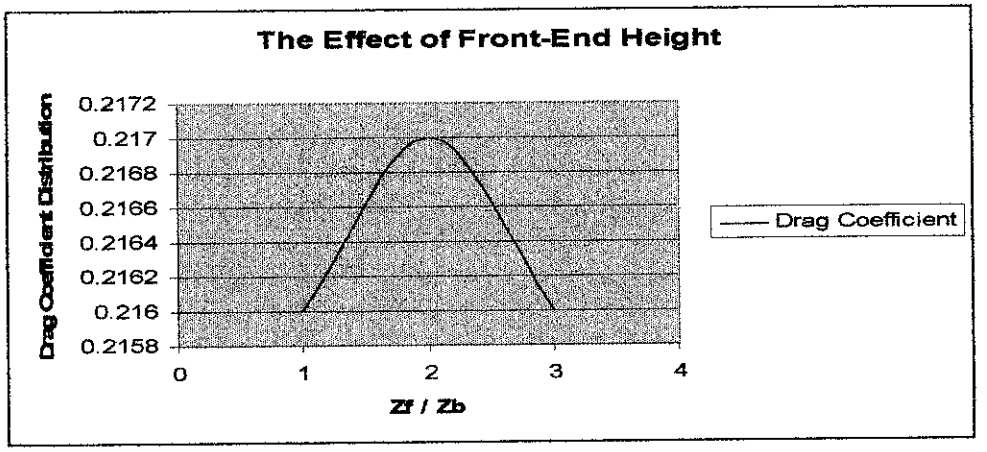

Graph 1: The effect of Front-End Height

The result shows the difference in drag coefficient for those three parameters. However, the different are very small and we can pick either design 1 or 3 as our model. The selected model will be used for further and complete aerodynamic analysis, in this model.

4.2.2 The Notchback Rear

In vehicle design, the generic type of rear geometry (i.e. hatchback, notchback, or squareback) is selected by the stylist, not the aerodynamicist. The choice is based on function and design theme, as well as aesthetics. The role of the aerodynamicist is to achieve low drag for the configuration that has been selected. Therefore, the notchback rear has been selected base on the HEV's configuration. The important thing that matter now is how to reduce the drag coefficient, C_D.

The important factor in notchback rear is the β, made by a line joining the rear end of the roofline to the tip of the boot (trunk). Another factor in notchback rear is α, the backlight angle. As shown in the graph *(Please refer Figure 18 in appendix II-I)*, the drag variation of this shape shows similarities to the drag variation of the hatchback (fastback). Theoretically, to get low β value, the boot (trunk) needs to be raised and/or lengthened. As a result, it will reduce the drag exerted at the back of the car. However, the α value does influence the drag exerted at that region as well. The best combination between these two angles will provide low drag coefficient value, C_D as well as the influence of decklid height on the drag coefficient (*Please refer Figure 19 in appendix II-I)*

This is another combination that can lead to low drag coefficient of a vehicle. In this experiment, the best parameter for decklid height must be selected first before proceeding to the best parameter of rear end tapering. However, the selected parameter must be within the acceptable dimension of the HEV's concepts.

4.2.3 Underbody Profiling

Most cars have the rough and disorderly underside that may lead to high C_D value. The floor-pan with a curved diffusing (pressure rising towards the rear) underside at the rear would provide low C_D value, as being shown in appendices *(Please refer Figure 20 in appendix II-II).*

The upsweep of the underside increases the rearward taper thus tending to reduce the form of drag. The high air-flow velocity will tend to reduce the pressure under the vehicle, thus providing the negative lift (down force) which is good for the car performance. A smooth underside profile will also provide a worthwhile reduction in surface friction drag.

4.2.4 The comparison between sharp and blunt body edges

Design 1 (sharp edges)

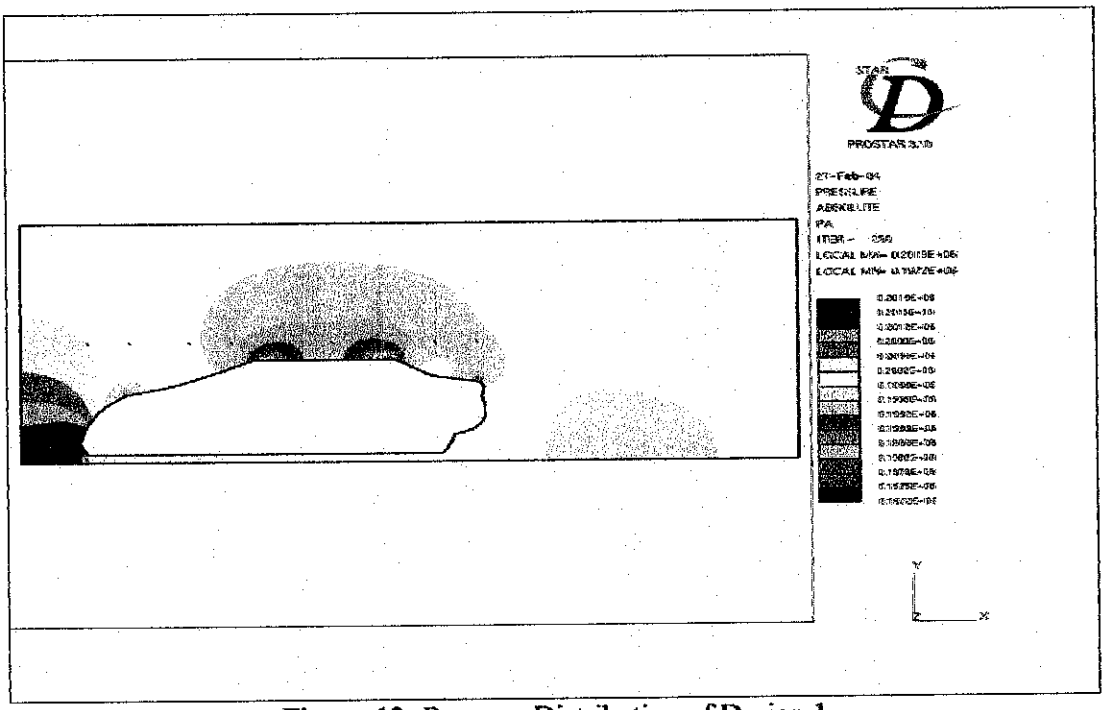

Figure 12: Pressure Distribution of Design 1

Pressure Coefficient

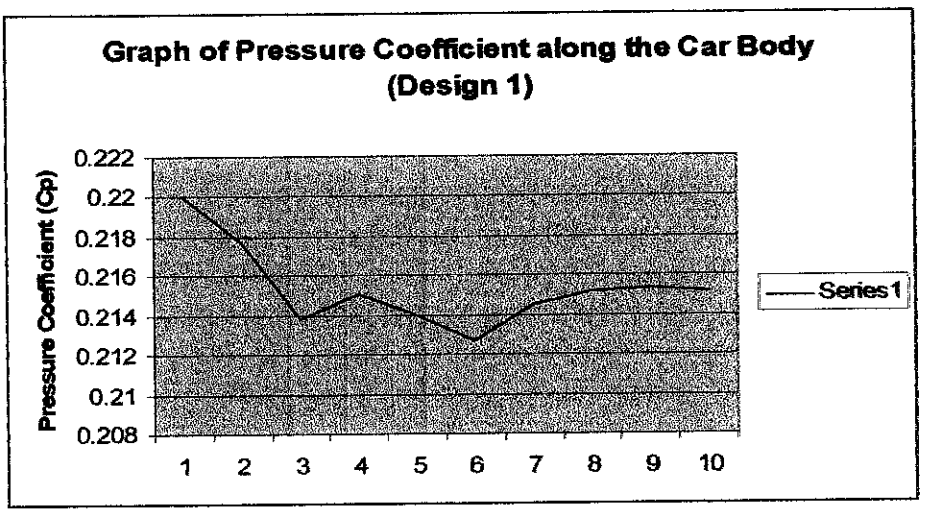

Graph 2: Graph of pressure coefficient (Design 1)

Design 2 (Blunt edges)

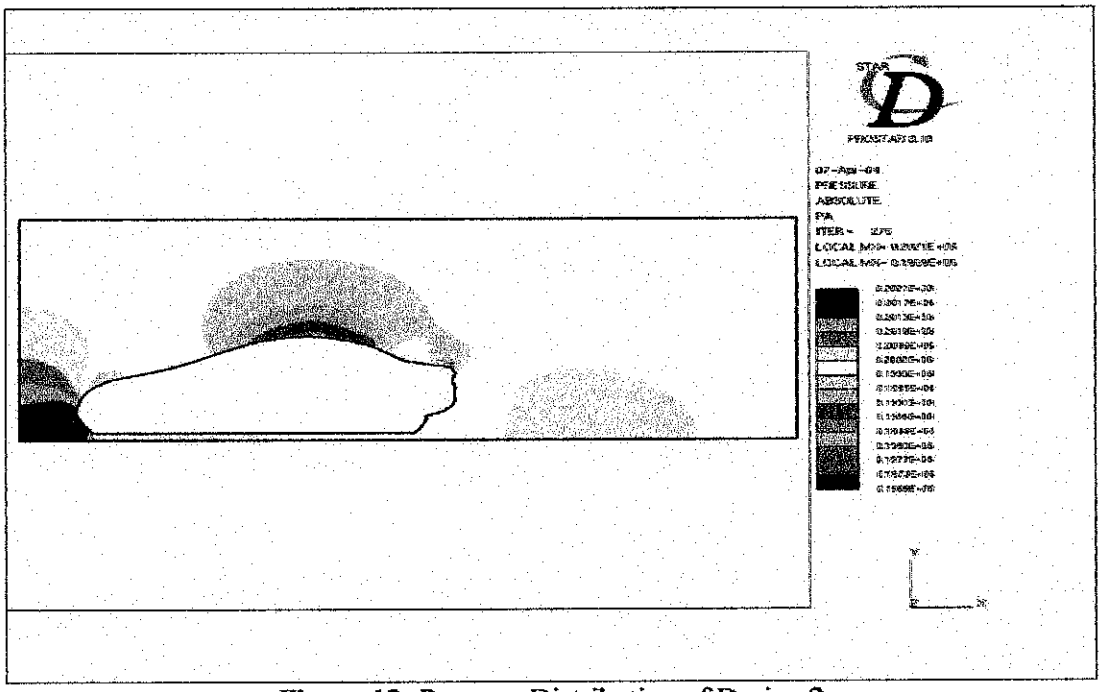

Figure 13: Pressure Distribution of Design 2

Pressure Coefficient

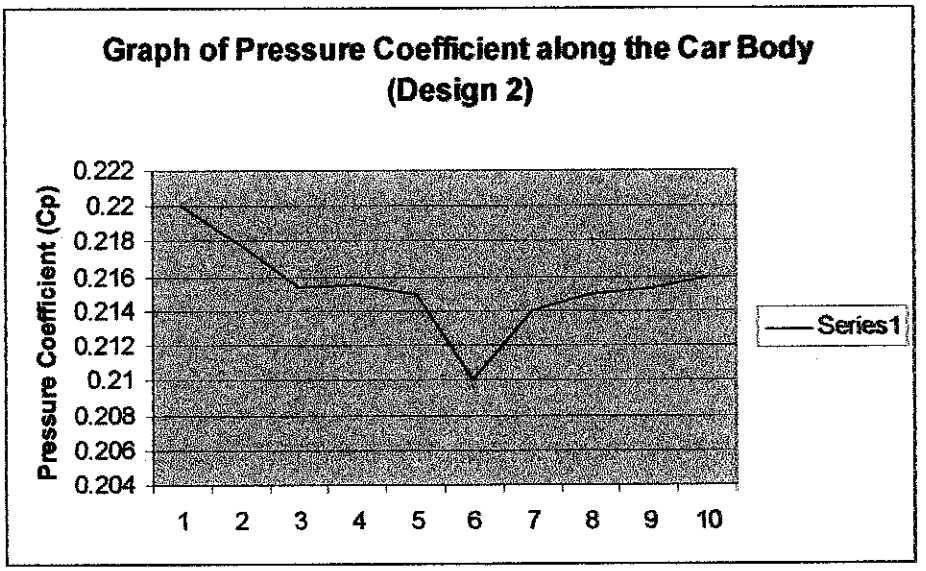

Graph 3: Graph of pressure coefficient (Design 2)

Both graphs (Design 1 & 2) show the pattern of pressure coefficient (Cp) acting on the body of the vehicle. The Cp is calculated from 20-30 pressure points taken along the vehicle's body, started just after the stagnation point and end at the rear of the vehicle. At the stagnation points in the flow (v = 0) the pressure coefficient Cp = 1. On the upper surfaces high pressure is found on the bonnet and windscreen (Cp > 0). However, at the top of the roof, the Cp values are still above 0. Theoretically, the values of Cp at this section should be negative (Cp < 0).

When refer back to the pressure distribution figure, the value of P on this section is still higher than the atmospheric (surrounding) pressure. This is due to the minimum separation area generated on this model. There is still an attachment of air flow when the airs travel over this section. When refer back to the drag coefficient theory/formula:

$$\overline{C_p} = 1/A \int_A C_p \, dA$$

And,

$$D_{np} = \tfrac{1}{2} \rho v^2_{atm} (\overline{C_{pf}} - \overline{C_{pr}})$$

Therefore,

$$C_{Dnp} = \frac{Dnp}{\tfrac{1}{2} \rho A v^2_{atm}} = (C_{pf} - C_{pr})$$

Base from this formula, the more positive C_{pr} (rear), the lower C_{Dnp} will be. The flows attachments have generated positive values of Cp for the rear section and we can aspect low C_D will be obtained for this model. The data of pressure tapping for both designs is available in the appendix III.

4.2.5 Sample Calculation

Pressure Coefficient (along the centerline of the vehicle):

$$C_p = \frac{P - P_{atm}}{\tfrac{1}{2} \rho v^2_{atm}}$$

$$C_p = \frac{(200.15 - 100)kPa}{\tfrac{1}{2} (1.205 kg/m^3) (27.78 m/s)^2}$$

$C_p = 0.2154$

Mean value of Cp (along the centerline of the vehicle):

$$\overline{C_p} = 1/A \int_A C_p \, dA$$

$$\overline{C_p} = 1 / 2.3545 \, [(0.22)(1.7)(0.14) + (0.22)(1.7)(0.38) + (0.21)(1.7)(0.22) + (0.22)(1.7)(0.18) + (0.21)(1.7)(0.38)]$$

$$\overline{C_p} = 0.20$$

Drag Coefficient (along the centerline of the vehicle):

$$C_{Dnp} = \frac{Dnp}{\frac{1}{2} \rho A v^2_{atm}} = (C_{pf} - C_{pr})$$

$$C_{Dnp} = 0.2 - 0.14 = 0.06$$

Theoretically, the correct value of drag coefficient of any vehicle (2-D analysis) can be obtained from the summation of the mean value of Cp (along the centerline) and the mean value of Cp (along the offset line from the centerline). The values obtained from this summation are acceptable and can be used in the design analysis. The values of C_D obtained in this report have been added with the $C_{D(offset)}$ value which is 0.08.

From the pressure coefficient graph, both designs acquired the same pattern of graph along the vehicle body. However, base on the drag coefficient calculation, the design 2 possessed lower C_D value compared to design 1:

Design 1; $C_D = 0.16$
Design 2; $C_D = 0.14$

Therefore, design 2 will be used for modeling and this design will be consider as the final design for this project.

4.2.6 Velocity Profile of the Final Design

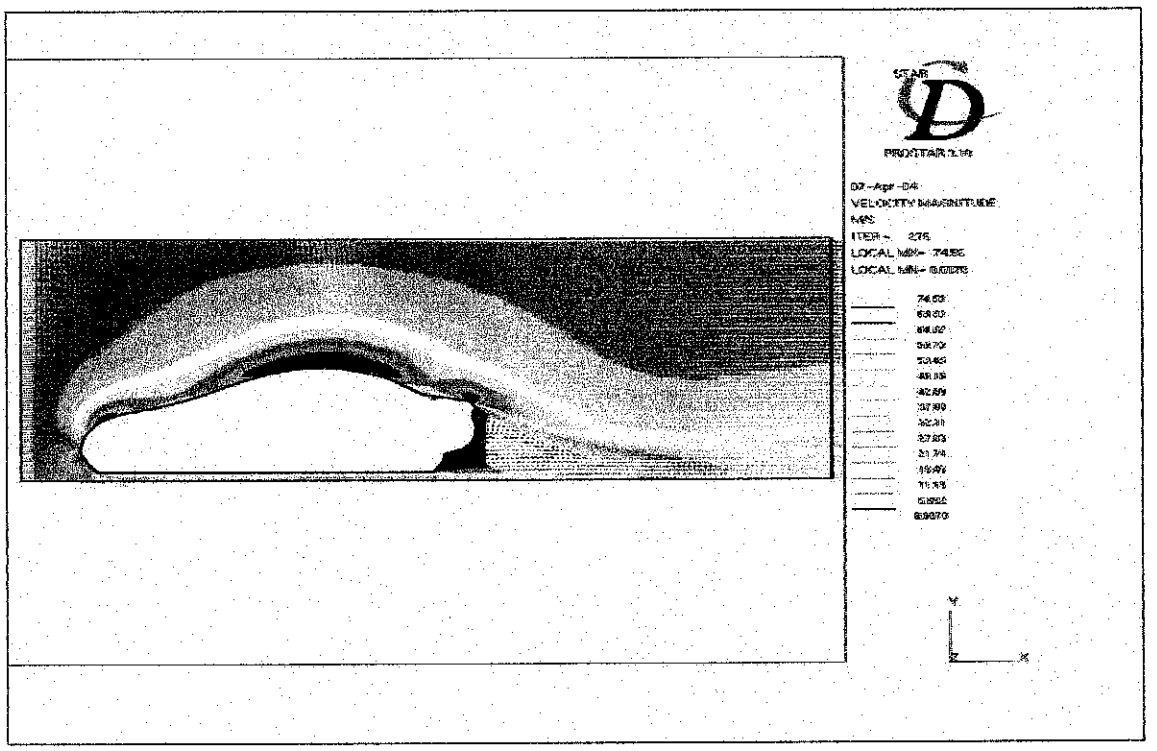

Figure 14: Velocity Profile of the Final Design

When refer to Figure above, we can see the flow profile acting on the surface of the vehicle. The air flows, along the upper surface of the vehicle and below the vehicle as well. The pattern of the flows shows that it is more likely the streamlined half-body at a ground plane. The theoretical value of drag coefficient for streamlined half-body at a ground plane is 0.09. When compared to the drag coefficient value obtained for this model, which is 0.16, it shows that the value is acceptable and this model is really a promising one.

From the figure below, separation started to occur from the edge of the front hood.

Figure 16: Velocity profile at the front end

After reattachment, the flows seem able to follow the shape of the vehicle's body until it reaches the top (roof) section. When refer back to the initial model, separation does occurred at the base of the front windscreen. The final design has eliminated the undesired condition and came out with more smooth flows on the vehicle.

Although the flow runs almost along the upper body surface in the experiment, the flow started to separate from the body surface at the roof end.

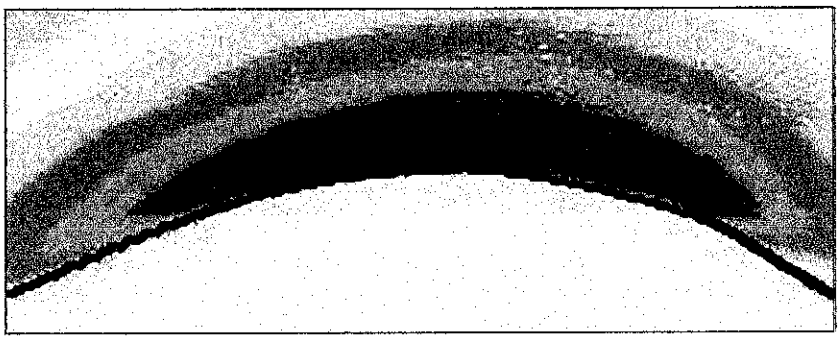

Figure 16: Velocity at the roof end

Partial and unsteady reattachment had occurred again at the rear edge of the trunk. The wake region is at the back of the vehicle. There was a large wake region formed due to the flow separation at the back of the vehicle. However, the counter rotating vertices is minimum when compared to any conventional notchback vehicle. This might be the main contribution to the low drag force exerted at the rear part of this model. The vertices decomposed constantly as it moved further away from the vehicle.

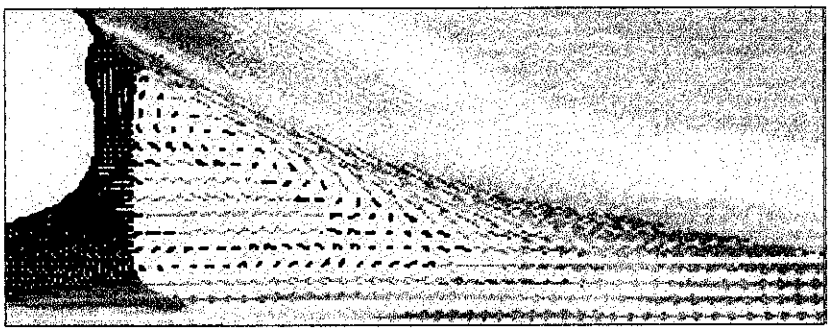

Figure 17: The wake region at the rear end

The flow separations are caused by strongly adverse pressure gradients (pressure increasing rapidly in the direction of the flow). From the pressure distribution, it may be seen that the separation positions correspond with regions of strongly adverse pressure gradient. Other drag-producing aspects of the flow around the vehicle are the conical vortices which are generated by separations from the A-post at the font, and at the rear. Removing such undesirable features is not particularly difficult and some modification (reducing) the backlight angle (angle between rear windscreen and trunk) and optimizing the underbody profiling were made and almost streamline body design is acquired. This has reduced the wake region formed at the back of the vehicle.

CHAPTER 5

CONCLUSION AND RECOMMENDATION

5. CONCLUSION AND RECOMMENDATION

The computational fluid dynamics (CFD) will plays an important role in the design analysis at this stage of the project. The reliability of this software was proven from the various analyses over different configurations around the car. With the combination of underbody profiling, front, and the most important part, rear end, the objective of this project could be achieved which is to design vehicle shapes that produce desirable flow characteristic. Furthermore, low drag coefficient (C_D) would be obtained as well.

The Computational Fluid Dynamics (CFD) analysis has been done continuously through the second semester of the final year project until the final design of the vehicle is acquired. The analysis had took much time than normal due to the time constraint since the author still has to focus on other courses taken in the respective semester. Furthermore, there are a lot of problems related to the 3-D drawing of the model and its have affected the simulation analysis. That is why all the computational fluid dynamic or the simulation analysis was done in 2-D approaches. However, the method used in determining the drag force and drag coefficient exerted on the model of vehicle is applicable and the results obtained are not much differed if compared to the 3-D analysis.

However, the 3-D computational fluid dynamic analysis consist the whole package of aerodynamic analysis. From 3-D modeling, all parts on the car including tires are taken into consideration. All the curvy parts at the side of the vehicle are being analyzed. This will lead to more accurate result of drag force exerted on the car. Additionally, the noise effect from vehicle aerodynamic can also being analyzed and better brand new design of a ground vehicle can be obtained. Base from the value of drag coefficient obtained in this whole project, it shows that this is a promising design. As a recommendation, a 3-D modeling of computational fluid dynamic

analysis based on the current model should be proposed to another new FYP student in order to come out with the finest brand new model of a vehicle ever made in UTP.

The trial and error experiments using wind-tunnel testing is not very practical for this project. The availability of the equipment itself and the cost constraint allocated for this project may be the main reason. In Malaysia, there are only several small scale wind-tunnels being built and the material used to build the mock-up models is quite costly. The trial and error experiments will involved a lot of possible models and each model need to be tested in the wind-tunnel. As a conclusion, a lot of money will be involved for traveling expenses and to build up the model. Therefore, base on the analysis and the result obtained, the computational fluid dynamics still can be rely on to do the external aerodynamic analysis over the vehicle body.

REFERRENCES

[1] Dr. V. Sumantran, and Dr. Gino Sovran; *Vehicle Aerodynamics*; SAE Int.; 1996.

[2] Julian Happian-Smith; *An Introduction to Modern Vehicle Design*; SAE Int.; 2002.

[3] R H Banard; *Road Vehicle Aerodynamic Design*; Longman; 1996.

[4] Computational Fluid Dynamics STAR-CD; Methodology; CD adapco Group; 2001.

[5] Computational Fluid Dynamics STAR-CD; Tutorials; CD adapco Group; 2001.

[6] Mohd. Arief; Automotive Systems; *Ground Vehicle Aerodynamics* (GVA2004.

[7] A.N. Stokes, X.-L. Luo, 1997-2003, CSIRO Australia <http://CMIS Research - Computational Fluid Dynamics - FEM Application.htm>.

[8] X.-L. Luo, A.N. Stokes and N.G. Barton; *Turbulent flow around a car body - Report of Fastflo solutions*; WUA-CFD Freiburg; 1996.

[9] R. Glowinski and O. Pironneau; *Finite element method for Navier-Stokes equations*; Annual Review of Fluid Mechanics, **24**,167-204; 1992.

[10] Klaus A. Hoffmann, Eulerio F. Toro, Mohamed M. Hafez, 2003 < http://Computational Fluid Dynamics - CFD.htm>.

[11] Vehicle aerodynamic simulation, 2003 <http://CD adapco Group - Group news.htm >.

[12] Vehicle aerodynamic simulation, 2003 <http://CD adapco Group - CFD products - es-aero- knowledge based Expert System for external aerodynamics.htm >.

[13] Brett Durie, Jason Elbot, Jen Panik, 2003 <http://beetle-refference.htm >

[14] American Iron and Steel Institute, 2003 <http://American Iron and Steel Institute Automotive Technical Information/Advanced Vehicle Concepts.htm >

[15] Peter Fretty, CLB MEDIA INC., 2001<http://Advanced Manufacturing - July 2001 - Automotive Materials.htm >

[16] Mr. William Z. Strang, Air Force Research Laboratory's Air Vehicles Directorate, 1999-2003 < http://www.afrl.af.mil/techconn/index.htm >

[17] Dr. Robert F. Tomaro, Dr. Matthew J. Grismer, and Mr. Frank C. Witzeman;Air Vehicles Directorate; 1999-2003.

[18] Karim Nice, 1998-2003 Howstuffworks, Inc <http://(Howstuffworks)HybridCars-Honda Insight.htm>.

[19] Karim Nice, 1998-2003 Howstuffworks, Inc <http://(Howstuffworks)HybridCars-Honda Insight.htm>.

[20] Paul Haney 1999, 2000 <http:// Howstuffworks-friction.htm>.

[21] Paul Haney 1999, 2000 <http:// Howstuffworks-Cd.htm >.

[22] Paul Haney 1999, 2000, 2001 < http://Howstuffworks-boundery layer.htm>.

APPENDICES

No.	Detail	Week															
		1	2	3	4	5	6	7	8	9	10	11	12	13	14	SW	EW
1	Selection of Project Topic																
2	Problem Definition & Design Goals																
3	Literature Review & Supplier Identification																
4	Submission of Preliminary Report																
5	Design Concepts & Analysis																
6	Economic Analysis/Budget																
7	CFD Modeling & Simulation																
8	Submission of Progress Report																
9	Wind Tunnel Testing																
10	Submission of Interim Report Final Draft																
11	Preparing Final/complete design																
12	Submission of Interim Report																

Project Milestone for First Semester of Final Year Project

Appendix I-1

No.	Detail	Week															
		1	2	3	4	5	6	7	8	9	10	11	12	13	14	SW	EW
1	Literature Review & Supplier Identification																
2	Submission of Progress Report 1																
3	Design Concepts & Analysis																
4	Economic Analysis/Budget																
5	CFD Modeling & Simulation																
6	Submission of Progress Report 2																
7	Wind Tunnel Testing																
8	Submission of Dissertation Report Final Draft																
9	Preparing Final/complete design																
10	Submission of Dissertation Report																
11	Oral Presentation																

Project Milestone for Second Semester of Final Year Project

Appendix I-II

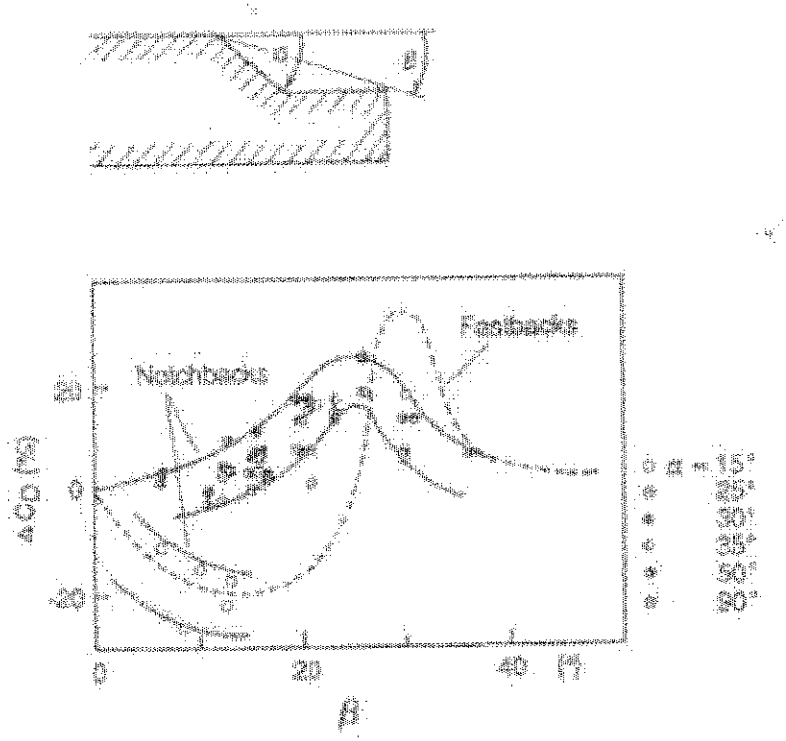

Figure 18: Dependence of drag on the afterbody geometry of notchbacks.

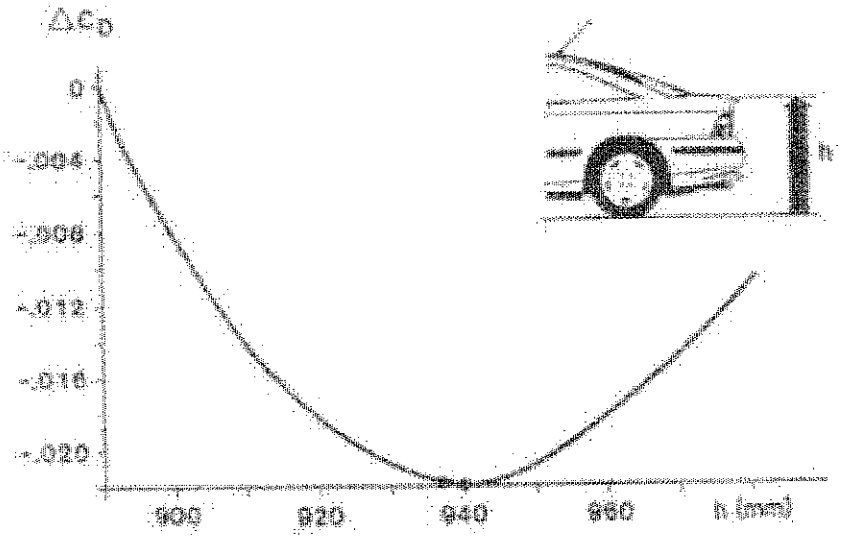

Figure 19: The influence of decklid height on the drag coefficient.

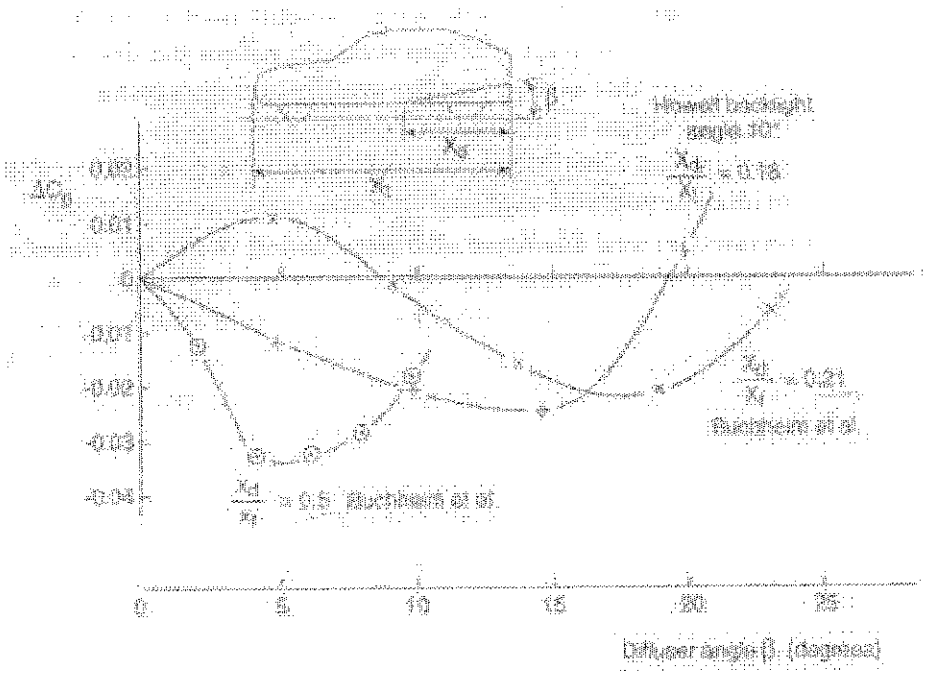

Figure 20: The effect of underbody tapering at the rear to produce a diffusing area.

Pressure Taps for Design 1 (front)

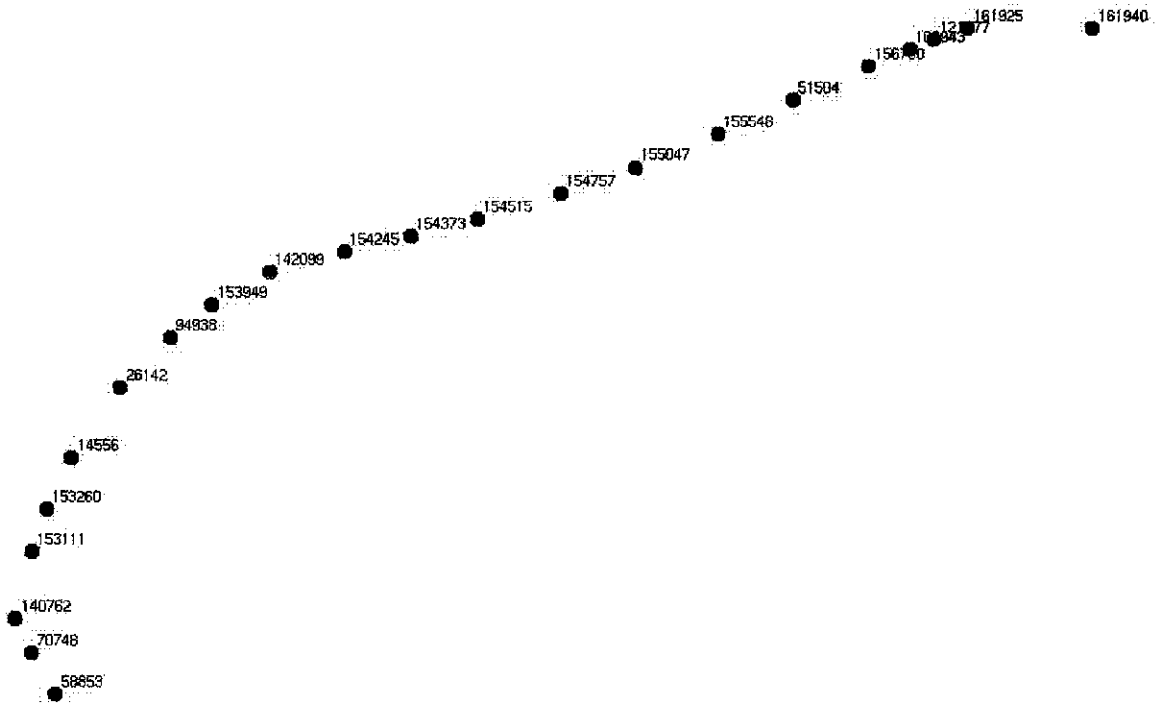

Data of Pressure Tabs (front)

Pressure Taps	Pressure (bar)
58853	199525
70748	201758
140762	201914
153111	201581
153260	201268
14556	200811
26142	200121
94938	199657
153949	199360
142099	198543
154245	199772
154373	200013
154515	200147
154757	200197
155047	200168
155548	200037
51504	199817
156780	199524
109943	199333
121777	199186
161925	198540

Pressure Taps for Design 1 (rear)

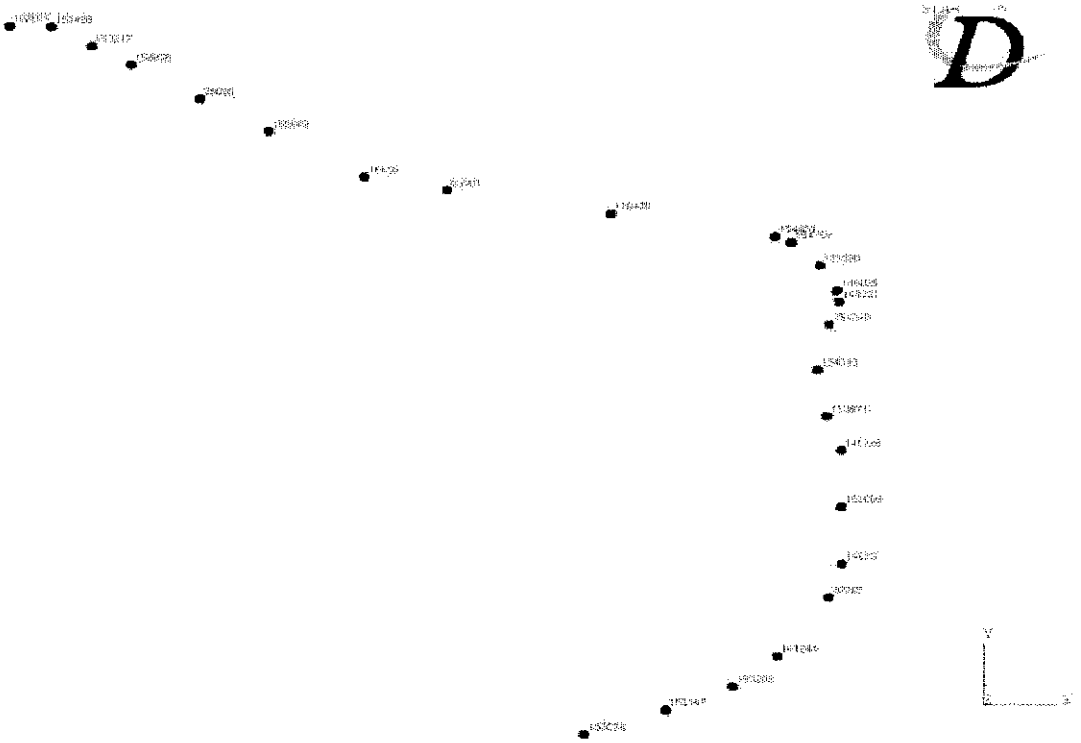

Data of Pressure Taps (rear)

Pressure Taps	Pressure (bar)
157498	198106
150217	199145
156956	199435
29086	199751
155982	200021
16655	200458
85001	200186
119470	199722
154851	198014
154759	197683
118990	199361
149823	199866
149821	199998
154248	200059
154039	200046
153871	200030
141726	200077
153609	200065
14635	200100
37305	200123
141244	200088
153208	200069
153147	200077
153076	200086

Pressure Taps for Design 2 (front)

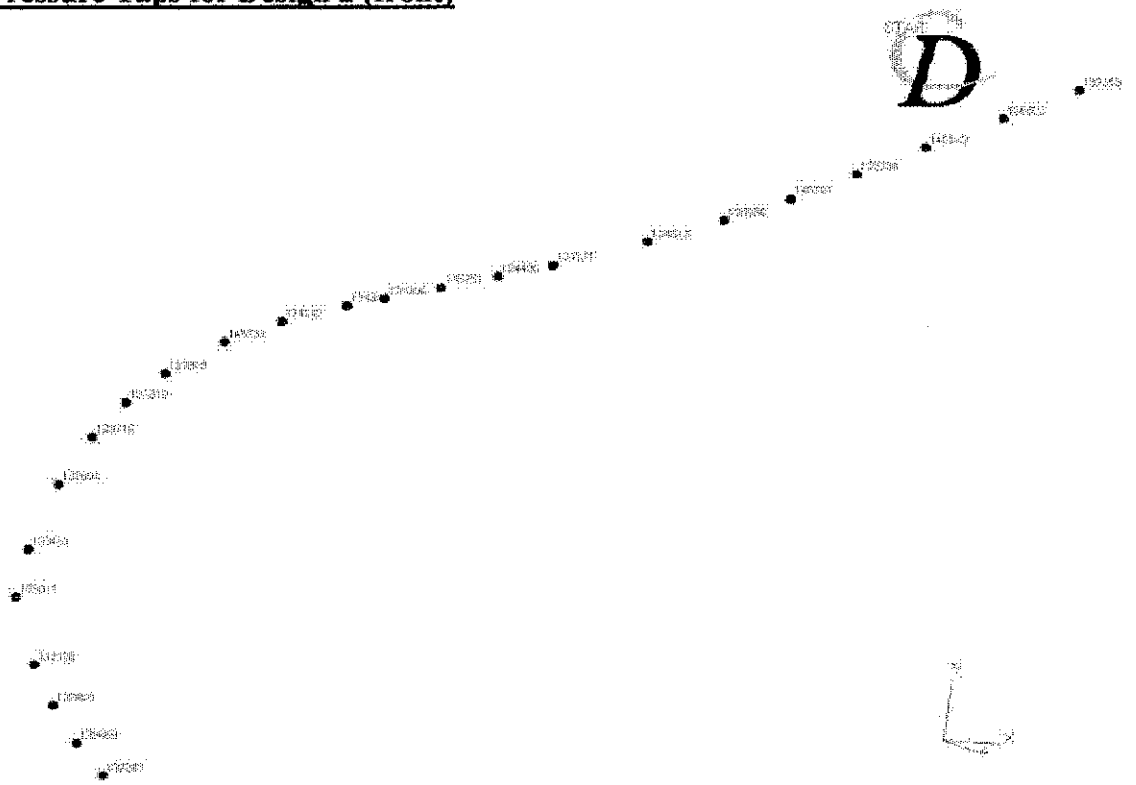

Data of Pressure Tabs (front)

Pressure Taps	Pressure (bar)
132268	199.542
132659	201.479
132860	201.881
133038	202.047
133311	201.822
133451	201409
133604	200642
133716	199966
133819	199518
133909	199217
145731	199131
134142	199317
134243	199764
134300	199885
145751	200024
134496	200137
134571	200217
134813	200269
135096	200257
145791	200204
135730	200092
145813	199913
136823	199681
137353	199430

Pressure Taps for Design 2 (rear)

Data of Pressure Taps (rear)

Pressure Taps	Pressure (bar)
139487	198727
139235	198764
138766	198800
145854	198806
137927	198233
145826	199689
135594	200622
135332	200115
135214	199809
135106	199325
134817	197929
145756	200097
134100	200141
145718	200129
145706	200143
145687	200170
133542	200175
145659	200132
133315	200139
133201	200148
132998	200144
132765	200137
132493	199970